Broadband THz Signals Propagate Through Dense Fog

Yihong Yang, *Student Member, IEEE*, Mahboubeh Mandehgar, and Daniel Richard Grischkowsky, *Fellow, IEEE*

***Abstract*— We experimentally demonstrate the propagation with minimal distortion and attenuation of broadband, complex THz signals through 137 m of dense fog with an approximate visibility of 7 m. The Mie scattering model is used to calculate the optical visibility, while the Rayleigh model is used to explain the observed THz attenuation.**

***Index Terms*— THz-TDS, atmosphere fog.**

I. Introduction

ADVANCED techniques, using propagating electromagnetic waves in the atmosphere, have attracted much attention due to their advantages of portability, easy-setup, low-cost and broad-band for many applications, such as infrared imaging, remote detection and Free Space Optics (FSO) wireless communications, covering frequencies from microwave to infrared and optics. However, suspended particles in the atmosphere, as in fog, smoke, clouds, dust and smog, can cause severe scattering, resulting in large variations in the received power and markedly limiting the service availability of FSO and infrared applications. Recent studies have indicated that the optical power losses for dense maritime fog and moderate continental fog extend up to 480 dB/km and 120 dB/km respectively [1], [2].

In contrast to this situation, broadband THz pulses can propagate through dense fog with much smaller propagation loss. For example, the attenuation due to optical Mie scattering (wavelengths smaller than the fog droplet diameters) by fog with a water content density of 0.1 g/m^3 is 100 dB/km [3], [4]. In contrast, the 500 GHz attenuation, in the Rayleigh limit (wavelengths much larger than the droplet diameters) is only 2.6 dB/km for the same density fog [5]–[7]. It is important to note that this attenuation is due to absorption by the water droplets, and not due to Rayleigh scattering, which is much smaller and can be neglected [5]–[7]. Here, we present experimental measurements that show, compared to the optical case, the reduction of THz loss in a fog is consistent with the above comparison. We will now discuss the scattering sizes in clouds, fogs, smoke and dust, in order to illustrate the opportunities for THz links.

Manuscript received August 1, 2014; revised November 13, 2014; accepted November 21, 2014. Date of publication December 2, 2014; date of current version January 21, 2015. This work was supported in part by the National Science Foundation.

The authors are with the School of Electrical and Computer Engineering, Oklahoma State University, Stillwater, OK 74074 USA (e-mail: yihong.yang@okstate.edu; m.mandehgar@okstate.edu; daniel.grischkowsky@okstate.edu).

Color versions of one or more of the figures in this letter are available online at http://ieeexplore.ieee.org.

Digital Object Identifier 10.1109/LPT.2014.2375795

With similar microphysical structure, both clouds and fog can be characterized by their water content (g/m^3), optical visibility and droplet size distribution. Maritime fog is an advection fog that forms when warm, moist air moves over colder water; the average droplet diameter is of order 20 μm [8]. Continental fog is a radiation fog, that forms inland at night, usually in valleys and low marshes and along rivers; it is generally characterized by droplets smaller than 20 μm in diameter [8]. Moreover, cumulus and stratus clouds have a droplet size distribution under the upper boundary of 50 μm [9], [10], and with the mean diameters less than 20 μm. The droplet number densities are in the range of 100–500 per cubic centimeter. The liquid water content is less than 1.0 g/m^3 for cumulus clouds) [9], [11]. Droplets with diameters larger than 50 μm become drizzle and increase in size during falling as rain [10].

In addition, several human activities, responsible for artificial cloud condensation nuclei, have been studied, such as, particles emitted from large paper mills [12], forest fires [13] and city pollution [14]. These effects can either broaden or narrow the cloud droplet size distributions in clouds from mean cloud droplet diameters of 20 μm up to 50 or down to 10 μm.

Several other types of particles may be suspended in the atmosphere to cause pollutions. For example, smog has particle sizes ranging from 0.003-6.8 μm [15]. The particle distributions from wood-smoke sources have a single mode that peaks between 0.1-0.2 μm particle diameter [16]. A parameterization for the global mineral aerosol size distribution into a transport model, using size classes between 0.1 and 50 μm has been developed [17]. The size classes are sand (particle diameters larger than 50 μm), silt (particle diameters between 2 and 50 μm), and clay (particles smaller than 2 μm). Since, the atmospheric lifetime of soil particles with diameters larger than 20 μm is less than a day, only smaller particles need to be considered for calculations of the radiative effects of dust.

Some works discussing fog and smoke effects on free space optical links [18] and far-infrared holograms [19] have been reported recently. However, there is still a lack of studies on the characteristics of broad-band THz pulse propagation through dense fog and smoke. In addition, the random variations in the refractive index from the atmospheric turbulence caused by temperature inhomogeneity and pressure fluctuations can cause scintillations for FSO and IR applications. Refractive index fluctuations can distort the coherent phase front of an IR light beam during passage through a few kilometers of atmosphere. THz beams are much less susceptible to scintillation effects, compared to IR beams.

1041-1135 © 2014 IEEE. Personal use is permitted, but republication/redistribution requires IEEE permission.
See http://www.ieee.org/publications_standards/publications/rights/index.html for more information.

The observed fog and cloud droplet size distributions are much less than the THz wavelengths (300 μm for 1 THz). Broadband THz signals can propagate through dense atmospheres of fog and clouds, because Rayleigh scattering can be neglected and the small attenuation is due to THz absorption by the water droplets. This situation presents the opportunity for THz applications such as imaging through dense fog, clouds and fire smoke, and high data rate wireless communication without interruptions.

Although atmospheric water vapor absorption attenuates propagating THz signals, a series of comprehensive, theoretical and experimental studies [20], has shown that for a 10 dB absorption loss, the corresponding THz signal propagation distances within the seven THz transparent windows, range from several hundred meters to several kilometers at RH 58% (10 g/m^3) and 20 °C.

II. Experiments

In this letter, we present THz-TDS experimental results of broad-band THz pulse propagation through a 137 m long path filled by a uniformly-distributed, dense, theater fog in a large cross-section, well-sealed sample chamber [21]. By controlling the concentration levels of fog inside the sample chamber, the direct measurements of fog effects, involve measuring the reshaped THz pulses and their relative transit times to a precision of $\pm$0.1 ps. The experimental results indicate that the broadband THz pulses show almost no effects from passage through a dense fog, which would be impenetrable for optical and IR beams.

The long-path THz propagation experimental setup is shown in Fig. 1(a) and described in [22] and [23]. The combination of a standard THz-TDS system with the long-path propagation setup, includes the controlled sample chamber, indicated by the red box in Fig. 1(a). A 12.5 μm thick sheet of plastic cling wrap covers the lab door, preventing fog from entering the lab. The total THz propagation path, including the 137 m path within the chamber, is approximately 170.5 m, equal to 51 laser pulses round trips of 3.3423 m in the mode-locked fs laser with a repetition rate of 89.6948 MHz [23]. The first optical pulse drives the transmitter Tx to produce the input THz pulse, which traverses the 170.5 m path, and is then measured by another optical pulse, delayed by 51 round trips in the mode-locked laser, driving the THz receiver Rx.

The theater fog used in the sample chamber is generated by a Hurricane 901 fog machine designed to make fog for theatrical productions. The water-based Chauvet Fog Fluid (FJU), with a specific gravity of 1.05, is a proprietary blend of 40% poly-functional alcohols with 60% water, being the main component. For our experiments, the FJU was diluted with water, 4 times the initial FJU volume, in order to increase the water percentage to 92% in the resulting fog.

The attenuation for optical Mie scattering by fog increases as the square root of the water density [3], [4]. For constant water density, the optical Mie scattering attenuation is inversely proportional to the droplet diameter [4].

For the THz Rayleigh model, Rayleigh scattering is negligible, and the comparatively much larger absorption by the

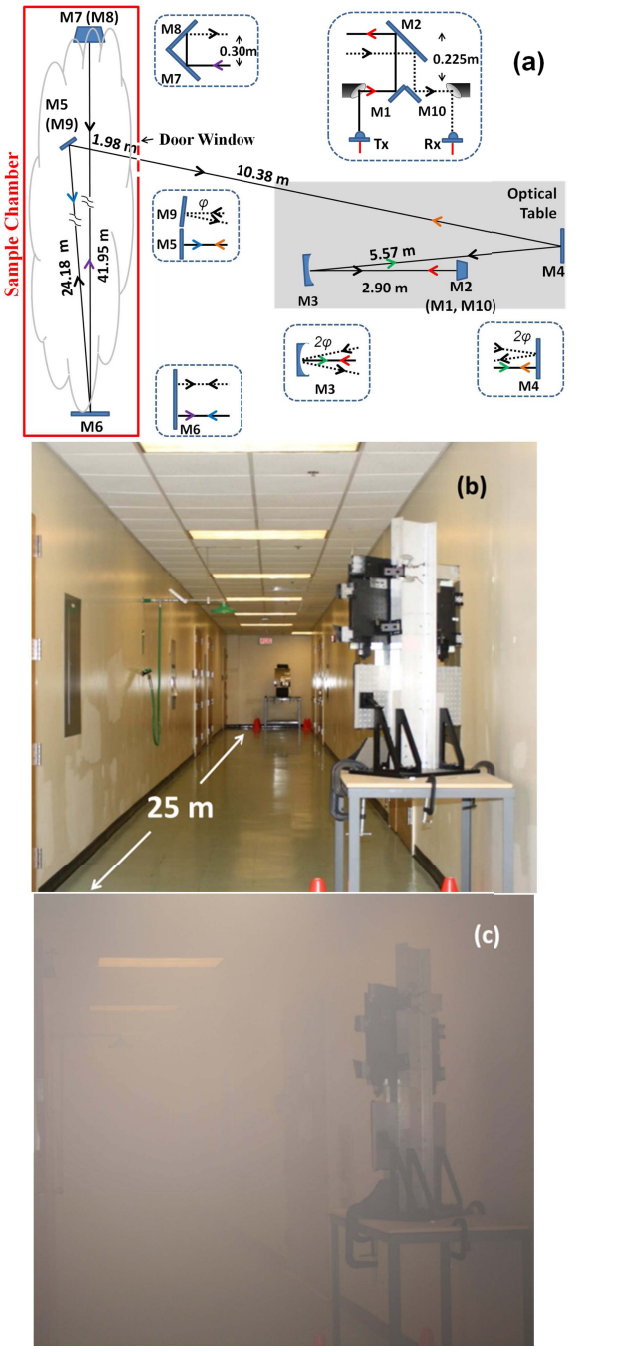

Fig. 1. (a) Experimental setup for 170.5 m long THz-TDS system with a sample controlled chamber (width 2.19 m, height 2.90 m, and length 43.09 m). (b) Photograph of clear-air chamber (25 m view from M5(M9) to M6). (c) Photograph of fog filled chamber.

water droplets of mm and THz waves, increases proportional to the water density [5]–[7]. In addition, for constant water density and for droplets much smaller than the wavelength, the Rayleigh attenuation is independent of the droplet diameter.

Figures 1(b)–(c) show the 25 m view from M5(M9) to M6 (illustrated in Fig. 1(a)) at one end of the clear-air chamber, before introducing the fog and the same view after 30 minutes of fog accumulation. It can be seen that, the dense fog reduces the visibility to approximately 7 m (the distance from M5(M9) to the first ceiling light), shown in Fig. 1(c).

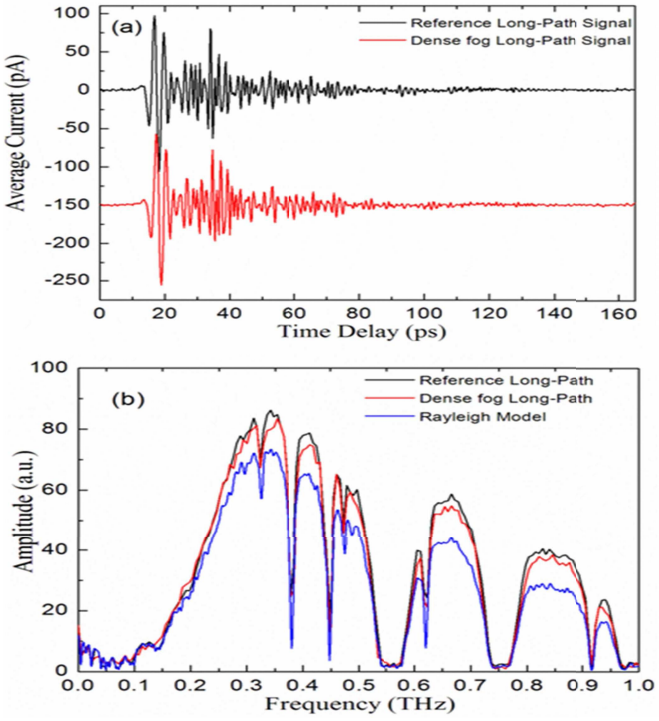

Fig. 2. First Measurement. (a) THz pulses transmitted through the 137 m sample chamber without fog (upper black trace) and with fog (lower red trace) corresponding to Fig. 1(b)–(c). (b) Corresponding amplitude spectra without fog (upper black line) and with fog (lower red line). Bottom (blue line) calculated transmitted spectrum through water fog (0.58 g/m^3) [5], [7].

The THz measurement process is the following: Firstly, several THz pulses transmitted through the sample chamber without fog are measured as reference pulses. The fog machine is then turned on for 30 minutes to accumulate heavy fog in the chamber, then the long-path THz dense fog pulses were measured. A set of input THz pulses with the standard THz-TDS system configuration (without M1 and M10) were taken at the beginning and end of the fog experiments, in order to monitor the stability of THz input pulses.

III. Discussion

The measured transmitted THz pulses and the corresponding amplitude spectra propagated through the long-path chamber (relative humidity RH 20% at 20 °C), without fog and with dense fog, corresponding to Fig. 1(b) and (c), are shown in Fig. 2(a) and (b). In our initial measurement, the highest fog concentration in the sample chamber reduced the visibility to approximately 7 m, as shown in Fig. 1(c). The transmitted THz fog pulse in Fig. 2(a), appears to be almost identical to the clear-air (no-fog) pulse with only the small 0.6 ps relative time shift between the two pulses.

In a repeat run of the measurements with better fog characterization, we measured a 10 minute half-life for the fog in the chamber, caused by both evaporation into water vapor within the chamber with humidity of 52% at 21 °C, and leakage from the chamber. The 1/e life-time for a stable analyte in the chamber has been measured to be 30 minutes. To achieve a stable dense fog with the measured spot-light, optical attenuation of 10 dB for a 10 m path within the chamber, required 50 minutes of fog production, which used

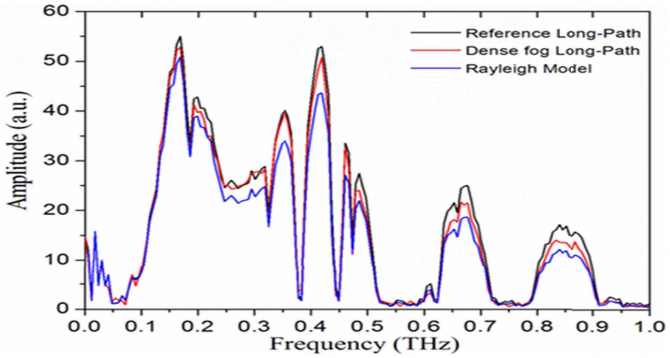

Fig. 3. Repeat measurements of the no-fog reference spectrum (top black line) transmitted through 137 m sample chamber, the measured fog transmission spectrum (middle red line), and the calculated transmitted spectrum (bottom blue line) through 137 m of water fog (0.58 g/m^3) [5], [7].

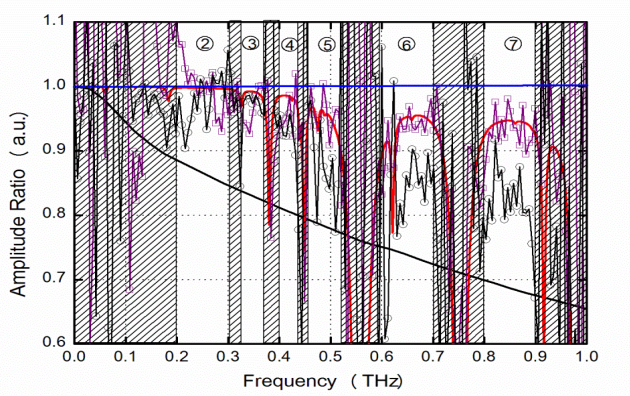

Fig. 4. Measured amplitude transmission (upper purple line) is the ratio of amplitude spectrum (with-fog) in Fig. 2b, to the spectrum without fog. Lower black line is the amplitude transmission for the repeat measurements of Fig. 3, for the corresponding ratio. The middle red line is the MRT calculated amplitude transmission for the water vapor density increase of 0.4 g/m^3. The lower smooth black line gives the calculated amplitude transmission for a fog with a 0.58 g/m^3 water density. The circled numbers mark the centers of the windows of transparency, which are the minimum loss regions between the strong water lines within the cross-hatched regions. These regions correspond to the maxima of the transmitted spectral amplitudes shown in Figs. 2(b) and 3 [22].

600 ml of dilute fog solution; the sample chamber volume is 300 m^3. The steady state fog density of 0.58 g/m^3, was 24% of the 2 g/m^3 density of the total fog produced.

The fog density of 0.58 g/m^3 would give a water fog optical loss of 243 dB/km with droplet diameters of 20 μm [3], [4], corresponding to a 10 m attenuation of only 2.43 dB. However, theater fog optically scatters much more than water fog, due to the smaller droplets, with diameters ranging from 1 to 2 μm. For our diluted 92% water solution, the diameters would be expected to be larger than 2 μm and smaller than the 20 μm for water fog. Assuming reasonable 5 μm diameters, the optical Mie scattering attenuation would increase to 972 dB/km in good agreement with the measurement.

The repeat measurements, shown in Fig. 3, compare the no-fog spectrum to the with-fog spectrum, and to the calculated spectrum for the attenuation of 0.58 g/m^3 of water fog [5], [7].

Figure 4 compares the measured amplitude transmissions of the first and repeat measurements with the Rayleigh loss transmission of 0.58 g/m^3 of water fog [5], [7].

For our initial measurement, the ratio of the transmitted amplitude spectra of the fog pulse to the no-fog pulse, shown in Fig. 2(b), gives the upper measured amplitude transmission curve in Fig. 4. The lower measured transmission is from the repeat measurement spectra in Fig. 3, with 10 dB optical attenuation for 10 m.

In Fig. 4, the upper first transmission is comparable to the calculated Molecular Response Theory (MRT) transmission through the additional water vapor (0.4 g/m^3) due to the fog evaporation, calculated from the fog production rate, the sample chamber leakage and the fog half-life. MRT reduces the far wings of the van-Vleck Weiskopf lineshapes [24].

As shown in Figs. 2–4, the monotonically decreasing transmission calculated by the Rayleigh model for a fog density of 0.58 g/m^3 [5]–[7], is significantly smaller than the measured total transmission, which also includes the absorption from the 0.4 g/m^3 additional water vapor due to fog evaporation. The fog calculation used analytic solutions [5], [7], and previous measurements of the complex index of refraction of liquid water from 0 to 1 THz [25].

As seen in Fig. 4, the predicted fog attenuation is significantly larger than the MRT calculation. The first (upper) transmission shows relatively good agreement with the MRT transmission over the entire range, while the repeat (lower) transmission is lower than the MRT transmission, but higher than for the water fog. Because the measured total transmissions in Fig. 4 include the extra water vapor MRT absorption and the fog absorption, the measured fog absorption is significantly smaller than the predicted fog absorption.

IV. Summary

Our high impact experimental results show that the THz spectral windows in fog are similar to the reference spectrum, without frequency shifts or additional resonant lines. According to these results, within an optically dense fog the performance of high speed THz wireless communication channels would be maintained [20], [26], as well as the transparent windows reserved for observation of finger print spectra in remote detection applications. The propagation of broadband THz pulses through a dense fog, shows that broadband THz waves could be also considered as a promising illumination source for many potential applications. For example, THz imaging through a dense fire smoke could guide fire-fighters to the safest path, as well as providing guidance through the extremely dense smoke of a forest fire. Another promising area would be to help the instrument landings for airplanes under severe conditions of fog, or smog, or volcano dust.

References

[1] M. Gebhart *et al.*, "Measurement of light attenuation in dense fog conditions for FSO applications," *Proc. SPIE*, vol. 5891, p. 58910K, Sep. 2005, doi: 10.1117/12.614830.

[2] B. Flecker, M. Gebhart, E. Leitgeb, S. S. Muhammad, and C. Chlestil, "Results of attenuation measurements for optical wireless channels under dense fog conditions regarding different wavelengths," *Proc. SPIE*, vol. 6303, p. 63030P, Sep. 2006, doi: 10.1117/12.680456.

[3] S. S. Muhammad, M. S. Awan, and A. Rehman, "PDF estimation and liquid water content based attenuation modeling for fog in terrestrial FSO links," *Radioengineering*, vol. 19, no. 2, pp. 228–236, 2010.

[4] M. S. Khan *et al.*, "Empirical relations for optical attenuation prediction from liquid water content of fog," *Radioengineering*, vol. 21, no. 3, pp. 911–916, 2012.

[5] K. Koester and L. Kosowsky, "Millimeter wave propagation in fog," in *Proc. Int. Antennas Propag. Symp.*, Los Angeles, CA, USA, Sep. 1971, pp. 329–332.

[6] H. J. Liebe, T. Manabe, and G. A. Hufford, "Millimeter-wave attenuation and delay rates due to fog/cloud conditions," *IEEE Trans. Antennas Propag.*, vol. 37, no. 12, pp. 1617–1623, Dec. 1989.

[7] S. Raghavan, *Radar Meteorology*. Dordrecht, The Netherlands: Kluwer, 2003, pp. 85–86.

[8] H. Vasseur and C. J. Gibbins, "Inference of fog characteristics from attenuation measurements at millimeter and optical wavelengths," *Radio Sci.*, vol. 31, no. 5, pp. 1089–1097, 1996.

[9] N. L. Miles, J. Verlinde, and E. E. Clothiaux, "Cloud droplet size distributions in low-level stratiform clouds," *J. Atmos. Sci.*, vol. 57, no. 2, pp. 295–311, 2000.

[10] J. G. Hudson and S. S. Yum, "Droplet spectral broadening in marine stratus," *J. Atmos. Sci.*, vol. 54, no. 22, pp. 2642–2654, 1997

[11] E. P. Shettle, "Models of aerosols, clouds and precipitation for atmospheric propagation studies," in *Proc. AGARD Conf.*, 1989, vol. 454, no. 15, pp. 1–13.

[12] R. C. Eagan, P. V. Hobbs, and L. F. Radke, "Particle emissions from a large kraft paper mill and their effects on the microstructure of warm clouds," *J. Appl. Meteorol.*, vol. 13, no. 5, pp. 535–552, 1974.

[13] R. C. Eagan, P. V. Hobbs, and L. F. Radke, "Measurements of cloud condensation nuclei and cloud droplet size distributions in the vicinity of forest fires," *J. Appl. Meteorol.*, vol. 13, no. 5, pp. 553–557, 1974.

[14] J. W. Fitzgerald and P. A. Spyers-Duran, "Changes in cloud nucleus concentration and cloud droplet size distribution associated with pollution from St. Louis," *J. Appl. Meteorol.*, vol. 12, no. 3, pp. 511–516, 1973.

[15] K. T. Whiteby, R. B. Husar, and B. Y. H. Liu, "The aerosol size distribution of Los Angeles smog," *J. Colloid Inter. Sci.*, vol. 39, no. 1, pp. 177–204, 1972.

[16] M. J. Kleeman, J. J. Schauer, and G. R. Cass, "Size and composition distribution of fine particulate matter emitted from wood burning, meat charbroiling, and cigarettes," *Environ. Sci. Technol.*, vol. 33, no. 20, pp. 3516–3523, 1999.

[17] I. Tegen and A. A. Lacis, "Modeling of particle size distribution and its influence on the radiative properties of mineral dust aerosol," *J. Geophys. Res.*, vol. 101, pp. 19237–19244, Aug. 1996.

[18] M. Ijaz, Z. Ghassemlooy, J. Pesek, O. Fiser, H. Le Minh, and E. Bentley, "Modeling of fog and smoke attenuation in free space optical communications link under controlled laboratory conditions," *J. Lightw. Technol.*, vol. 31, no. 11, pp. 1720–1726, Jun. 1, 2013.

[19] M. Locatelli *et al.*, "Imaging live humans through smoke and flames using far-infrared digital holography," *Opt. Exp.*, vol. 21, no. 5, pp. 5379–5390, 2013.

[20] Y. Yang, M. Mandehgar, and D. Grischkowsky, "THz-TDS characterization of the digital communication channels of the atmosphere and the enabled applications," *J. Infr., Millim., Terahertz Waves*, doi: 10.1007/s10762-014-0099-3.

[21] Y. Yang, M. Mandehgar, and D. R. Grischkowsky, "Measurements of broadband THz pulse propagation through dense fog," in *Proc. CLEO*, Jun. 2014, pp. 1–2, paper SF1F5.

[22] Y. Yang, M. Mandehgar, and D. Grischkowsky, "Broadband THz pulse transmission through the atmosphere," *IEEE Trans. THz Sci. Technol.*, vol. 1, no. 1, pp. 264–273, Sep. 2011.

[23] Y. Yang, M. Mandehgar, and D. Grischkowsky, "Time domain measurement of the THz refractivity of water vapor," *Opt. Exp.*, vol. 21, no. 24, pp. 26208–26218, 2012.

[24] Y. Yang, M. Mandehgar, and D. Grischkowsky, "Determination of the water vapor continuum absorption by THz-TDS and molecular response theory," *Opt. Exp.*, vol. 22, no. 4, pp. 4388–4403, 2014.

[25] J. Zhang and D. Grischkowsky, "Waveguide terahertz time-domain spectroscopy of nanometer water layers," *Opt. Lett.*, vol. 29, no. 14, pp. 1617–1619, 2004.

[26] M. Mandehgar, Y. Yang, and D. Grischkowsky, "Atmosphere characterization for simulation of the two optimal wireless terahertz digital communication links," *Opt. Lett.*, vol. 38, no. 17, pp. 3437–3440, 2013.